LEGIBILITY NOTICE

A major purpose of the Technical Information Center is to provide the broadest dissemination possible of information contained in DOE's Research and Development Reports to business, industry, the academic community, and federal, state and local governments.

Although a small portion of this report is not reproducible, it is being made available to expedite the availability of information on the research discussed herein.

A-UR-88-3328

LOCF-8809119--3

Alamos National Laboratory is operated by the University of California for the United States Department of Energy under contract W-7405-ENG-36

TITLE: **NEW PHOTOELECTRIC INJECTOR DESIGN FOR THE LOS ALAMOS NATIONAL LABORATORY XUV FEL ACCELERATOR**

LA-UR--88-3328

DE89 002044

AUTHOR(S): B. E. Carlsten

SUBMITTED TO: 10th International Free-Electron Laser Conference, Jerusalem, Israel, August 29-September 2, 1988

DISCLAIMER

Los Alamos
s Alamos National Laboratory
s Alamos, New Mexico 87545

NEW PHOTOELECTRIC INJECTOR DESIGN FOR THE LOS ALAMOS NATIONAL LABORATORY XUV FEL ACCELERATOR*

B. E. CARLSTEN

Los Alamos National Laboratory, MS-H825, Los Alamos, NM 87545 (U.S.A.)

The injector for the Los Alamos National Laboratory XUV FEL accelerator has been redesigned to provide more charge to the wiggler. The new design can deliver 8 nC of charge within 20 ps with a normalized 90% emittance of <25 π·mm·mrad to the wiggler at an energy of 200 MeV. In addition to the new design of the injector, we analyze the emittance growth and subsequent reduction through the injector, including the different mechanisms for emittance growth and the methods used to eliminate the correlated emittance.

1. Introduction

As has been reported before [1, 2], Los Alamos National Laboratory proposes to construct an XUV FEL system, extending from 1 to 400 nm, as a user's facility. In a previous paper [1], two preliminary rf linac injector and accelerator designs were presented that met minimum quality values for the electron beam [2]. The first design started with a photoelectric injector and used magnetic bunching to obtain high peak currents. The second design, meant as a backup, started with a conventional thermionic Pierce gun and also relied on magnetic bunching. The emittance from the second design, although more than 50% larger than from the first design, still was below the minimum emittance requirement for lasing at 50 nm.

There were several reasons to redo the design using the photoelectric injector. First, only 2.5 nC of charge was available at the wigglers (about 250 A), which is only marginally larger than the minimum of 2 nC. The beam was filtered by an aperture at relatively low energy, which could generate deleterious wakefields. Also, from the experimental program at Los Alamos National Laboratory, we learned that magnetic bunching is very dangerous [3]. In addition to the wakefields reported in that reference, beam emittance is affected by the potential depression as the beam is bunched and also by higher order (sextupole and up) nonachromatic transport components in the bend. In addition, magnetic bunchers are sensitive to energy jitter in the accelerator, resulting in arrival time jitter at the wigglers. For these reasons, we redesigned the accelerator using a photoelectric injector without magnetic bunching or an aperture for filtering. Computer simulations

*Work supported by the Division of Advanced Energy Projects of the US Dept. of Energy, Office of Basic Energy Science, and the Los Alamos National Laboratory

were done with the particle-pushing code PARMELA. In the earlier review, beam breakup and other instabilities were studied for the 1.3-GHz cavities used; the study will not be repeated here.

In sect. 2, we will review the electron beam requirements determined from theoretical FEL interaction studies.

In sect. 3, we will analyze the emittance growth mechanisms in the injector and show how it is possible to achieve extremely low emittances. Design considerations resulting from this analysis will be used in sect. 4 to generate an alternative photoelectric design, still with good emittance, but with 8 nC delivered to the wiggler.

2. Electron beam requirements

Simulations of the free-electron lasing interaction have indicated the following minimum quality values for an electron beam entering an undulator [1]:

Wavelength	50 nm	12 nm	4 nm
Energy	250 MeV	500 MeV	750 MeV
Normalized 90% emittance	≤ 40 π·mm·mrad	≤ 24 π·mm·mrad	≤ 4 π·mm·mrad
Peak current	≥ 100 A	≥ 150 A	≥ 200 A
Energy spread (FWHM)	≤ 0.2%	≤ 0.1%	≤ 0.1%

The required micropulse charge is at least 2 nC within these specifications.

The proposed facility will have a series of FEL oscillators through which the electron beam will pass sequentially (fig. 1). The oscillators requiring better electron beam quality are first in the sequence. There will be slight energy extraction from the electron beam in each of the oscillators, hence only slight beam quality degradation. Thus if the electron beam satisfies the requirements for the first oscillator, the beam will still have sufficient quality by the time it reaches any of the latter oscillators to satisfy their less stringent requirements too.

All emittances quoted in this paper refer to the normalized phase-space areas occupied by 90% of the beam's particles. Thus if the beam has a waist with radius r_0 and maximum divergence angle r_0', the emittance will be slightly less than $\gamma \pi r_0 r_0'$.

3. Emittance analysis

There are four mechanisms in the injector that contribute to emittance growth:

- Linear space charge
- Nonlinear space charge
- Nonlinear time-independent rf
- Linear time-dependent rf

We will examine each one of these mechanisms in turn. We will show that the first one will dominate, but can be eliminated completely, and that the residual emittance will primarily be due to a tradeoff between the second and fourth ones.

3.1 Linear space charge

This is the most important mechanism, so this part will comprise the bulk of this paper. In fig. 2 we see a typical emittance plot as a function of distance down the linac for a typical simulation for an 8-nC, 20-ps pulse in a 1.3-GHz photoinjector. We see an immediate emittance growth to about 100 π·mm·mrad and subsequent reduction to a minimum of about 25 π·mm·mrad at a location z_f downstream. The location of z_f can be pushed arbitrarily far away, and at a sufficiently high energy there is essentially no emittance growth after that location. We will show, in this section, how this emittance growth and reduction occurs with a simple model. We will study a drifting slug beam (fig. 2); the effects of rf acceleration and rf focusing will be shown to be a variation in the definition of the space charge force $m_o\lambda$, the distances z and z_l, and the initial size and divergence of the slug. For convenience we will also define an internal coordinate system ρ and ζ to indicate different points in the slug beam, with $\rho = r_o$ defining the initial radial size. In fig. 2 we define points B to represent the axial edges for $\rho = r_o$ and points A for the center at $\rho = r_o$. We let the slug beam drift a distance z_l to a lens and a distance z after the lens.

The emittance growth mechanism that is due to linear space charge [which we will define in eq (6)] has been outlined before [4] for a drifting beam. However, the physics is very different after focusing with a lens, as we will show.

First we will examine the effect of constant space charge. We will call this the weak focusing limit. This case with zero initial beam divergence has a solution that is consistent with a well-focused beam downstream, which is not true in general. We assume the space-charge force $m_o\lambda$ is a function only of ρ and ζ and not of z. The edge of the beam initially at location (r_o, ζ) will obey

$$r(\zeta) = r_o + \lambda(r_o, \zeta)\, z_l^2/2$$

$$r'(\zeta) = \lambda(r_o, \zeta)\, z_l$$

at the lens. If we assume $\lambda(\rho, \zeta) = (\rho/r_o)\,\lambda(\zeta)$, we obtain a laminar beam, although this is not required for the subsequent development. We next assume a linear lens at position $z = 0$ of focal length $1/\alpha_L$. Then at position z the beam edge obeys

$$r(\zeta) = r_o + \lambda(\zeta)(z_l + z)^2/2 \cdot \alpha_L [r_o z + \lambda(\zeta)\, z_l^2\, z/2]$$

$$r'(\zeta) = \lambda(z_l + z) \cdot \alpha_L (r_o + \lambda(\zeta)\, z_l^2/2) \qquad (1)$$

In fig. 3, we examine the phase space plots corresponding to different axial locations. We observe in (d) that the emittance is different from the emittance in (c). This difference is because the relative velocity between points A and B varies between (c) and (d) by

$$\Delta(x'_A - x'_B) = z\,[\lambda(A) - \lambda(B)]$$

Because of this effect we can reduce the emittance. It is important to remember this is only possible because the space charge varies for different particles. In fact with

$$a_L = 2\,\frac{z_1 + z}{z^2} \quad , \tag{2}$$

we obtain

$$r(Q = \frac{z + 2z_1}{2z}\,(\lambda(Q\,(z^2 - z_1^2) - 2\,r_o) \quad ,$$

and (3)

$$r'(Q = \frac{z_1 + z}{z^2}\,(\lambda(Q\,(z^2 - z_1^2) - 2\,r_o) \quad ;$$

therefore,

$$\frac{r'(Q}{r\,(Q} = \frac{2\,(z_1 + z)}{z(z + 2\,z_1)} \quad , \tag{4}$$

which is not a function of either λ or ζ. This is an important result because now at z the emittance has been reduced to zero because all points lie along a line at the same orientation in phase space.

There are two major regimes to examine. The beam can either make a waist or a crossover (fig. 4) depending on the relative strengths of the lens and the space charge. By using eq. (2) in eq (1) we obtain

$$\frac{2r}{\lambda}\,z = (z^2 - z_1^{\,2} - 2r_o/\lambda)\,(z + 2z_1) \quad .$$

The three solutions for $r = 0$ are

$z = z_{crit}$

$z = -z_{crit}$

$z = -2z_1$

where we define

$$z_{crit}^2 = z_1^2 - 2r_o/\lambda \quad .$$

Because we are only concerned with $z > 0$, only the first solution is important. From eq (3) we see that for $0 < z < z_{crit}$, $r < 0$ and for $z > z_{crit}$, $r > 0$. Thus we have two regimes: a crossover will occur for $z < z_{crit}$, and one can show only a waist will occur for $z > z_{crit}$. Thus our analysis is only valid for $z > z_{crit}$, because we assumed a constant space-charge force. The analysis fails if there is a crossover: in fact the analysis can only show that there is a solution and cannot predict if it occurs before or after the crossover. We will examine this regime later with a more general form for the space charge.

For validity of the space charge approximation, the beam must always be nearly the same size. In particular, the beam must undergo a waist, but also must not expand much beyond it. Thus, we must obey

$$z = z_{crit}(1 + \varepsilon) \tag{5}$$

where ε is about 1/10 or so.

The above analysis can be extended for general space charge as long as the beam expansion is self-similar, meaning that the ratio of the space charge forces at two points in the beam is a constant, or

$$\frac{d}{dz}\left(\frac{\lambda(\rho_1, \zeta_1)}{\lambda(\rho_2, \zeta_2)}\right) = 0 \quad . \tag{6}$$

Typically, λ is a function of the radius of the beam; thus,

$$r'' = \frac{d^2 r}{dz^2} = \lambda(r, \rho, \zeta)$$

Equation (7) is in general hard to integrate. However, if the beam expansion is self-similar,

$$\lambda(r, \rho, \zeta) = k(\rho, \zeta)\,\lambda(z) \quad ;$$

thus,

$$r'' = k(\rho, \zeta)\,\lambda(z) \quad . \tag{7}$$

Integrating with boundary condition $r'(-z_1) = 0$,

$$r = r_o + k \int_{-z_1}^{z} \int_{-z_1}^{z_2} \lambda(z')\, dz'\, dz_2$$

and

$$r' = k \int_{-z_1}^{z} \lambda(z')\, dz'$$

up to the lens; then

$$r = r_o + k\left(\int_{-z_1}^{z} \int_{-z_1}^{z_2} \lambda(z')\, dz'\, dz_2 + z \int_{-z_1}^{0} \lambda(z')\, dz'\right)$$

$$-a_L z\left(r_o + k \int_{-z_1}^{0} \int_{-z_1}^{z_2} \lambda(z')\, dz'\, dz_2\right)$$

and

$$r' = k\left(\int_{-z_1}^{z} \lambda(z')\, dz'\right) - a_L\left(r_o + k \int_{-z_1}^{0} \int_{-z_1}^{z_2} \lambda(z')\, dz'\, dz_2\right)$$

after it. These equations, similar to eq. (1), are of the form

$$r = A + Bk - a_L(C + Dk)$$

$$r' = E + Fk - a_L(G + Hk)$$

where all the ρ, ζ dependency is in k. The only solutions for a_L for zero emittance at z satisfy

$$0 = a\,a_L^2 + b\,a_L + C$$

where

$$a = -DG + CH$$

$$b = BG - AH - CF + DE$$

$$c = AF - BE$$

For this case,

$$a = 0$$

$$b = r_o \int_0^z \int_{z_1}^{z_2} \lambda(z')\, dz'\, dz_2 - r_o' z \int_o^z \lambda(z')\, dz'$$

$$c = r_o \int_{-z_1}^{z} \lambda(z')\, dz'$$

and

$$\alpha_L = \frac{\int_{z_1}^{z} \lambda(z')\, dz'}{z \int_o^z \lambda(z')\, dz' - \int_o^z \int_{z_1}^{z_2} \lambda(z')\, dz'\, dz_2} \quad , \tag{8}$$

which reduces to eq. (4) in the weak focusing limit. Thus, as long as the beam expansion is self-similar (eq. 6), eq 7 holds which leads to the unique solution for the lens' strength , eq. (8).

A solution exists for an initial divergence of the beam. In that case, with the weak focusing limit,

$$\alpha_L = \frac{(r_o - \frac{1}{2} r_o' (z_1 + z))(z_1 + z)}{\frac{z^2}{2} (r_o + r_c' z_1)} \quad .$$

From eq (8), we know a solution occurs, but in general we don't know if it is before or after a beam crossover. We will next examine the case of a crossover with constant space charge before $z = 0$ and

$$r'' = \frac{\lambda}{|z_x - z|}$$

for $z > 0$ with $\alpha_L = -1/z_x$ indicating a focus at $z = z_x$. For this model one can show that a solution exists for both $z < z_x$ and also $z > z_x$ for non-zero r_o'. Although this is not a regime that one wants to operate in (because a crossover will introduce nonlinear space charge emittance growth), it is unusual because there are two minimum emittance locations.

One can also show for the weak focus model with initial divergence r_o' that for $z_1 = 0$ and $r_c' > 0$, if

$$r_o = z^2 \lambda/2 + r_o' (3/2) z \quad ,$$

one solution occurs before and a second one after the waist.

With rf acceleration and focusing, z, z_1, λ, r_o and r'_o take on different values. With rf acceleration, new functions λ' and z' are defined by

$$\lambda' = \lambda/\gamma^2(z)$$

$$dz' = dz/\gamma(z)$$

because the transverse acceleration goes $1/\gamma^3$. An explicit form for the emittance with rf acceleration can be derived by integrating the above two equations [5]. If we assume a linear constant focusing field for the rf without acceleration, we can replace eq. (1) for r by

$$r = \frac{\sin(\sqrt{a}\, z)\,\frac{a_L}{\sqrt{a}}\,[\lambda\,(1-\cos(\sqrt{a}\, z_1)] + r_o\, a \cos(\sqrt{a}\, z_1)}{a\,[1-\cos(\sqrt{a}\,(z-z_1)]} \tag{9}$$

where a_L is the usual lens constant and a is a distributed focusing term so that

$$r'' = \lambda - r\,a \ .$$

Including the focusing a effectively changes the values of r_o, λ and r_o' to use. This will be examined in more detail in another paper [5]. In general, we know that if a is a function of z, a solution still exists from the linear nature of the equations, but is is hard to write an explicit formula for a_L. If $a(z)$ is piecewise constant, a solution of the form of eq. (9) in a series is possible. In fact, any function $a(z)$ can be represented sufficiently well by a series of piecewise constant values, if the intervals are taken sufficiently close together. A computer can aid in this type of analysis.

If the beam expansion is sufficiently self-similar, then we can write an explicit solution for a_L. If

$$r'' = k(\rho,\zeta)\,\lambda(z) - (\rho/\rho_o)\,a(z) \ ,$$

then

$$a_L = N/M$$

where

$$N = (r_o - \int_{-z_1}^{z}\int_{-z_1}^{z_2} a(z')\,dz'\,dz_2)\Big(\int_{-z_1}^{z}\lambda(z')\,dz'\Big) + \Big(\int_{-z_1}^{z}\int_{-z_1}^{z_2}\lambda(z')\,dz'\,dz_2 + \int_{-z_1}^{0}\lambda(z')\,dz'\Big)\int_{-z_1}^{z} a(z')\,dz'$$

and

$$M = r_o\Big(z\int_0^z \lambda(z')\,dz' - \int_0^z\int_{-z_1}^{z_2}\lambda(z')\,dz'\,dz_2\Big) + \int_{-z_1}^{0}\int_{-z_1}^{z} a(z')\,dz'\,dz\Big(\int_{-z_1}^{z_2}\int_{-z_1}^{z}\lambda(z')\,dz'\,dz$$

$$+ z\int_{-z_1}^{0}\lambda(z')\,dz'\Big) + z\Big(\int_{-z_1}^{0}\int_{-z_1}^{z_2}\lambda(z')\,dz'\,dz_2\int_{-z_1}^{z} a(z')\,dz' - \int_{-z_1}^{z}\int_{-z_1}^{z_2} a(z')\,dz'\,dz_2\int_{z_1}^{o}\lambda(z')\,dz'\Big)$$

$$- \int_{-z_1}^{o}\int_{-z_1}^{z_2} a(z')\,dz'\,dz_2\int_{-z_1}^{z}\lambda(z')\,dz'\Big)$$

3.2 *Nonlinear Space Charge*

Nonlinear space charge effects cannot in general be removed. Thus for the weak focusing limit, the criterion of eq. (5) must be used to minimize the non-self-similar beam expansion. As you will see in sect. 4, with this criterion, the nonlinear space charge still are not negligible. In addition to non-self-similar beam expansion, nonlinear space charge can occur from beam divergences and convergences. With a beam angle of θ, the emittance grows like

$$\varepsilon = 2 \quad \sqrt{2} \; \lambda \, \theta \, z \quad \sqrt{\frac{L^2}{24} + \frac{\theta^2}{r_o^2} \frac{L^4}{80}}$$

for a drift of length z and a bunch of length L. The first term is a constant for any angle, but the second term grows for larger θ.

3.3 *Nonlinear, time-independent rf fields*

This term refers to the nonlinear component in the rf fields, i.e., the component that deviates from

$$E_r(r,z) = E_o(z)\, r \cos(\omega t + \phi) \quad . \tag{10}$$

An earlier work has calculated cavity shapes for linear rf fields for sufficiently low frequencies that the electrostatic solution can be used [6]. An extension to electromagnetic fields is possible and necessary; at 1.3 GHz the nonlinearity of the fields contribute something like 15 π·mm·mrad to the normalized 90% emittance.

3.4 *Linear, time-dependent rf fields*

For one of the cases we will consider in sect. 4, the emittance of 15 π·mm·mrad arises from a combination of 11 π from the nonlinear space-charge effect and 11 π from the linear, time-dependent rf fields for a pulse of 20 ps. This last effect occurs from the time dependency of the rf fields. We assume the rf fields obey eq. (10). Then the emittance resulting from the time dependency goes as [7]

$$\varepsilon \sim E_o r^2 L$$

where r is the radius of the beam and L is its length. The physical size of the beam can be reduced to make these effects smaller until the nonlinear space-charge forces appear. With zero charge in the beam, it is possible to eliminate this effect with a third-harmonic cavity following each linac section because there will be no radial mixing. However, with space charge, the radial mixing destroys the correlation before the third-harmonic cavity. To reduce this effect with space charge, either a third-harmonic component must be introduced into each of the first couple of cavities or the constant E_o must be reduced for each one. E_o can be reduced by proper selection of the parameters μ and ψ in the linear field solution extension of [6] for electromagnetic fields.

4. Photoelectric injector design

Using the above analysis as a guide, we were able to design a robust injector for an XUV FEL with 8 nC of charge within 20 ps. In fig. 5 we see the design and the PARMELA simulation output corresponding to it. The results are well within the requirements outlined in sect. 2.

The cavities used for the simulation in fig. 5 are ones currently in use at Los Alamos. They are somewhat nonlinear; the final emittance of 23 π·mm·mrad resulted from half nonlinear rf fields and nonlinear space charge. We artificially linearized the rf fields to observe the benefit. It allowed us to enlarge the beam radius and drop the nonlinear space charge part until it was equal to the contribution from the linear-time-dependent rf. The overall emittance was then 15 π·mm·mrad. If we enlarged the beam further to eliminate all traces of the nonlinear space charge, the linear, time-dependent rf part grew to 18 π·mm·mrad. This is how we would like to operate the injector if at this point we could remove the linear-time-dependent rf contribution by one of the techniques discussed above.

5. Conclusion

A photoelectric injector design analysis has been presented. The emittance growth from the dominant mechanism has been shown to be eliminated with a simple lens configuration, leaving only a small residual emittance resulting from the other mechanisms. This analysis can lead to general design considerations including electrostatic and rf focusing, which is addressed in another paper [5]. The new photoelectric injector design shows very low emittance for 8 nC, and the leading remaining contributors to that emittance have been identified. Techniques to reduce this emittance further have been outlined.

6. Acknowledgments

I wish to acknowledge helpful discussions with Lloyd Young, Richard Sheffield, and Michael Jones, who pointed out that the rf contribution to the emittance is very small.

References

[1] B. E. Carlsten and K. C. D. Chan, "Preliminary Injector, Accelerator, and Beamline Design for RF-Linac-Driven XUV Free-Electron Lasers," Ninth Int. FEL Conf., Williamsburg, VA, September 14-18, 1987, to be published.

[2] J. C. Goldstein and B. D. McVey, "Recent Theoretical Results from an RF-Linac-Driven XUV Free Electron Laser," Proc. of the Eighth Int. Conf. on Free Electron Lasers, Glasgow, Scotland, September 1-5, 1986.

[3] B. E. Carlsten, D. W. Feldman, A. Lumpkin, W. E. Stein, J. E. Sollid, and R. W. Warren, "Emittance Studies at the Los Alamos National Laboratory Free Electron Laser," Ninth Int. FEL Conf., Williamsburg, VA, September 14-18, 1987, to be published.

[4] M. E. Jones and B. E. Carlsten, "Space-Charge Induced Emittance Growth in the Transport of High-Brightness Electron Beams," Proc. 1987 IEEE Particle Accelerator Conference, IEEE Catalog No. 87CH2387-9, 1319 (1987).

[5] B. E. Carlsten and R. L. Sheffield, "Photoelectric Injector Design Considerations," 1988 Linear Accelerator Conference, Williamsburg, VA October 3-7, 1988, to be published.

[6] M. E. Jones and W. Peter, "Particle-in-Cell Simulations of the Lasertron," IEEE Trans. Nucl. Sci. **32** (5), 1794 (1985).

[7] M. E. Jones and W. Peter, "Theory and Simulation of High-Brightness Electron Beam Production from Laser-Irradiated Photocathodes in the Presence of dc and rf Electric Fields," Los Alamos National Laboratory document LA-UR-86-1941, Proc. 6th Int. Conf. on High-Power Particle Beams, Kobe, Japan, June 1986, to be published.

Figure Captions

Fig. 1. Configuration of the proposed Los Alamos XUV/UV FEL (1 to 400 nm). One rf linear accelerator drives multiple FEL oscillators in series.

Fig. 2. Typical transverse emittance versus beamline position plot for a photoelectric injector, showing quick initial growth and subsequent reduction for a slug beam and physical description of a slug beam, with internal coordinates ρ and ζ.

Fig. 3. Transverse phase-space plots showing emittance growth and reduction.

(a) initial phase-space plot with very small emittance.

(b) phase space plot after drift z_1 to lens, showing the emittance growth due to the different expansion rates of points A and B.

(c) phase space plot immediately after lens, showing rotation due to the lens. The emittance is unchanged because we assume the lens is linear.

(d) phase space plot after drift z behind lens, showing the emittance reduction due to the different expansion rates of points A and B.

Fig. 4. Definition of a crossover and a waist. The solid line is the initial transvrse phase space distribution and the dotted line is the final distribution.

(a) A crossover is formed when converging particles cross the r' axis while transforming to diverging particles.

(b) A waist is formed when converging particles cross the r axis while transforming to diverging particles.

Fig. 5. Photoelectric injecor design of first few accelerator tanks and corresponding PARMELA output showing energy spread and emittance as a function of energy.

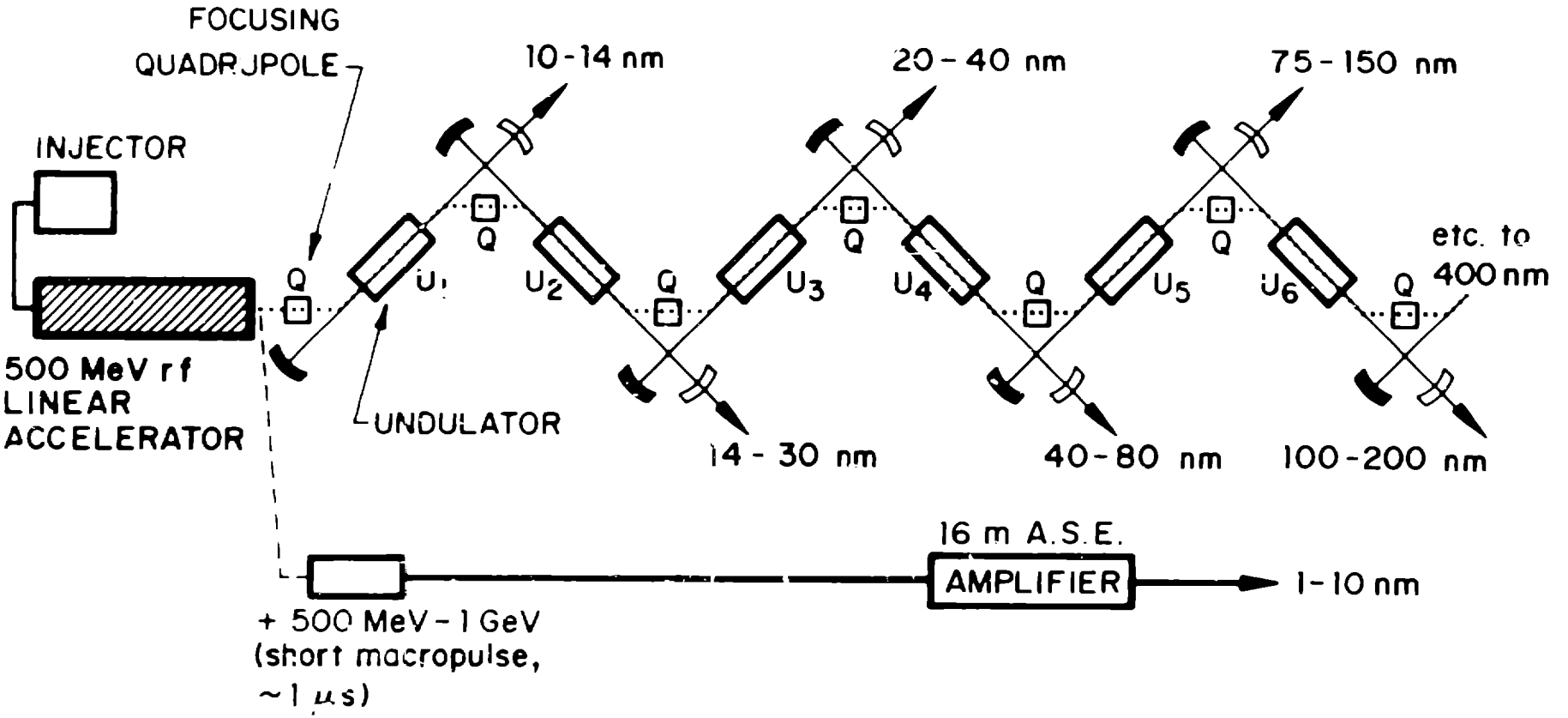
FOCUSING
QUADRUPOLE
INJECTOR
500 MeV rf
LINEAR
ACCELERATOR
Q
U1
UNDULATOR
10 - 14 nm
Q
U2
Q
14 - 30 nm
20 - 40 nm
Q
U3
Q
U4
40 - 80 nm
75 - 150 nm
Q
U5
Q
U6
Q
etc. to
400 nm
100 - 200 nm
16 m A.S.E.
AMPLIFIER
1 - 10 nm
+ 500 MeV - 1 GeV
(short macropulse,
~1 μs)

CHM-VG-4638-D

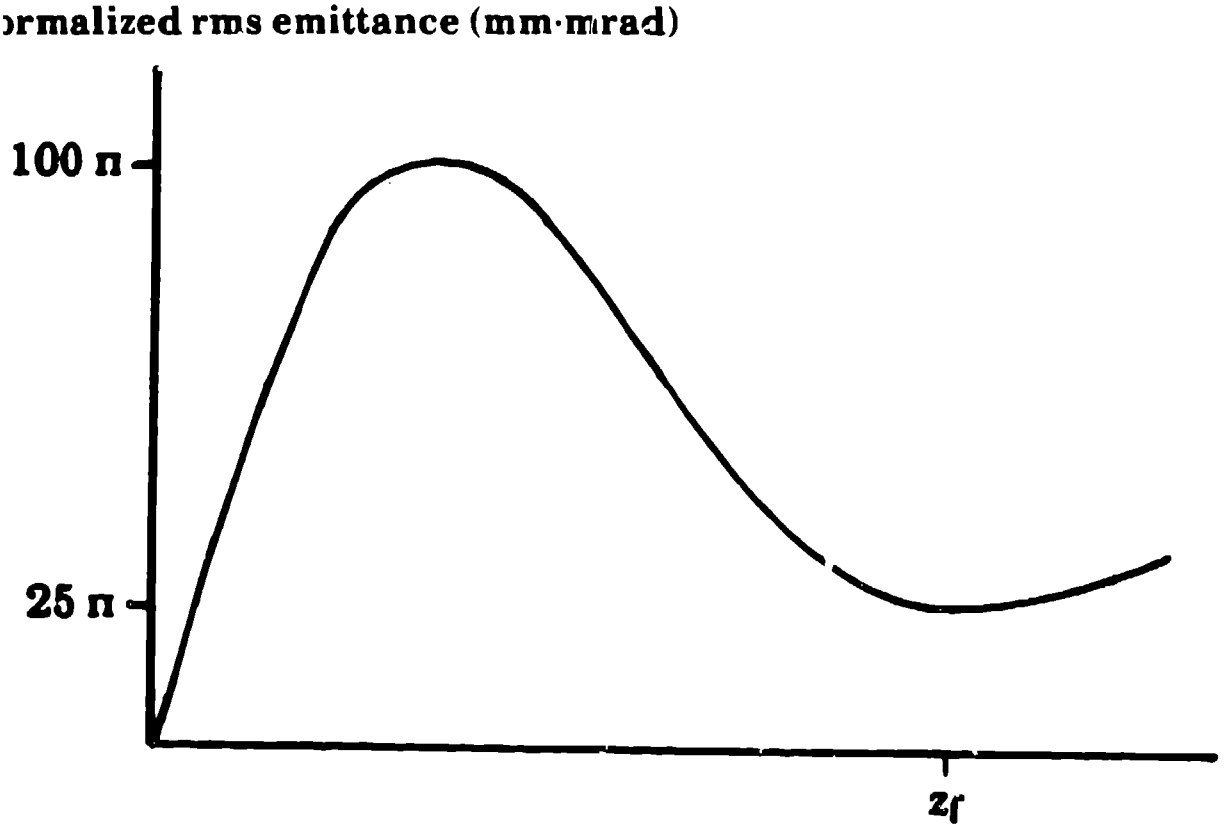

Typical emittance plot as a function of distance down the linac 8-nC, 20-ps pulse in a 1.32-GHZ photoinjector

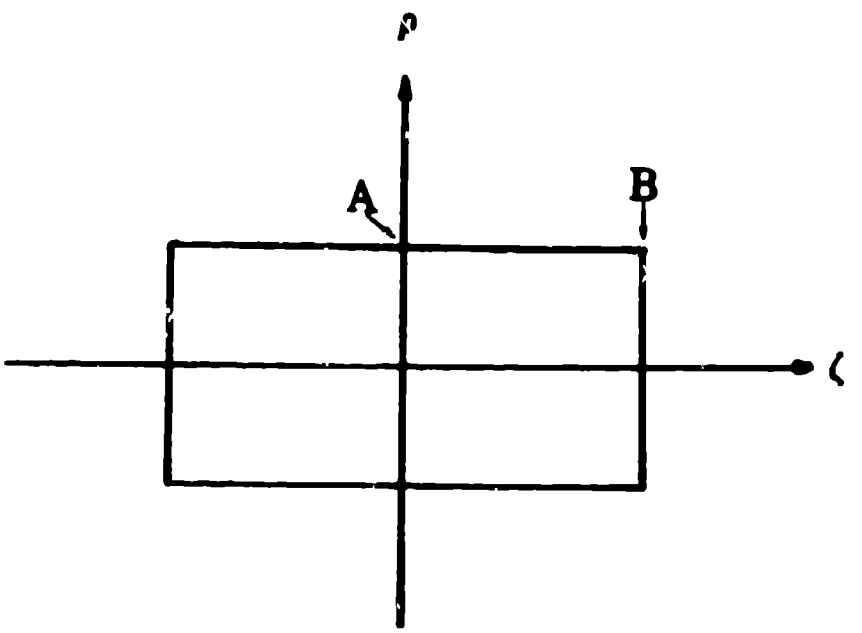

Drifting slug-beam internal coordinate system

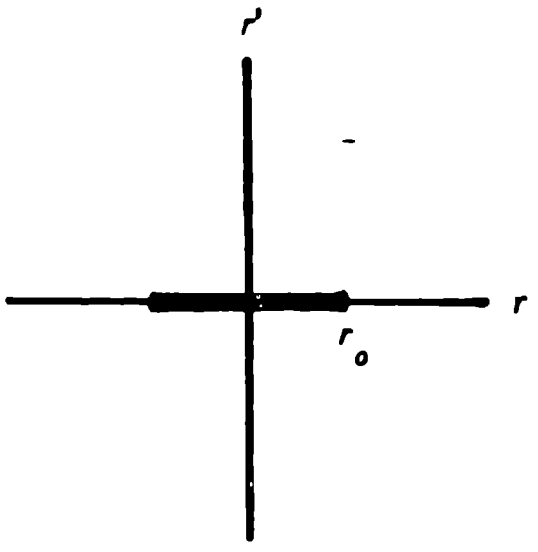

(a)

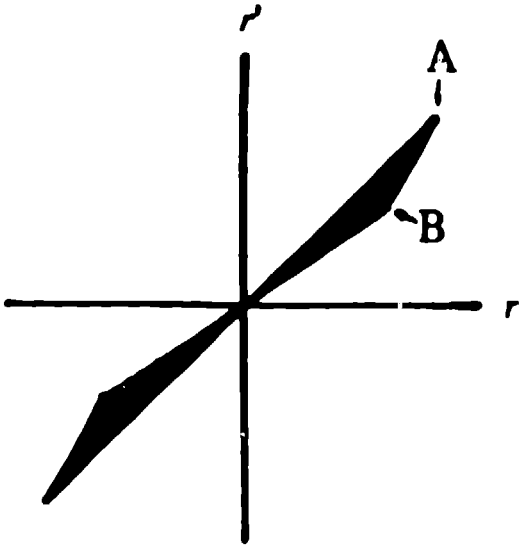

(b)

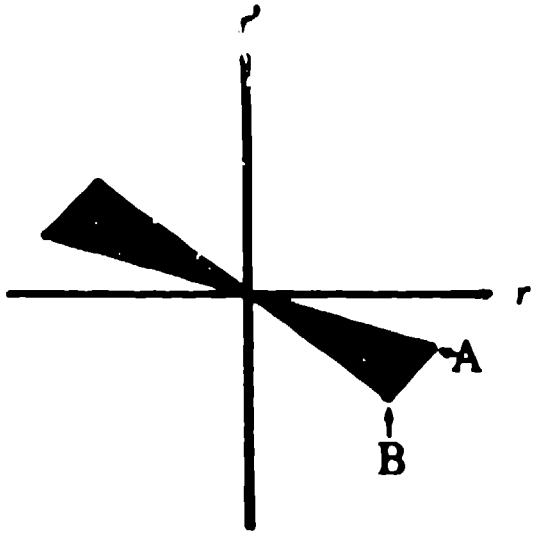

(c)

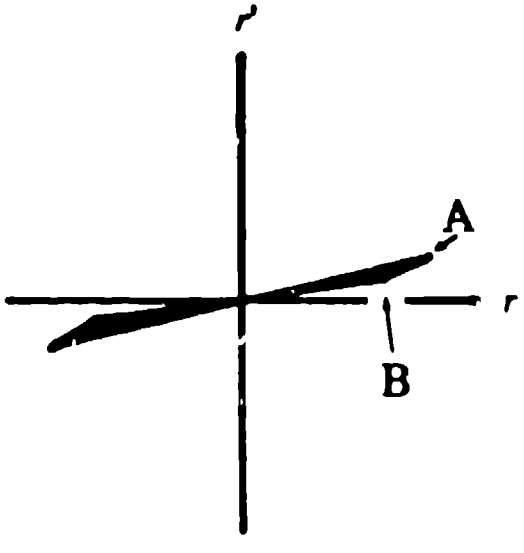

(d)

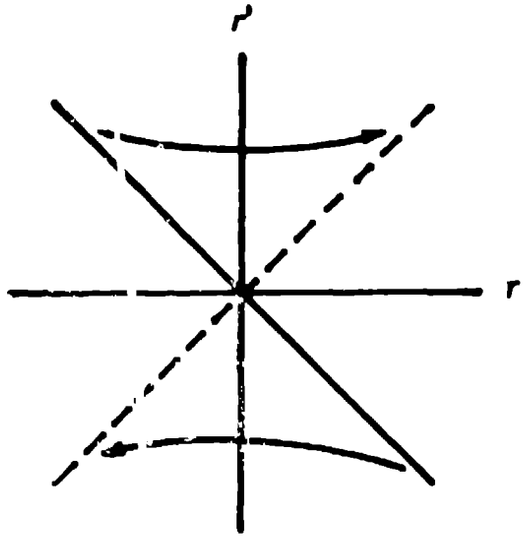

(a)

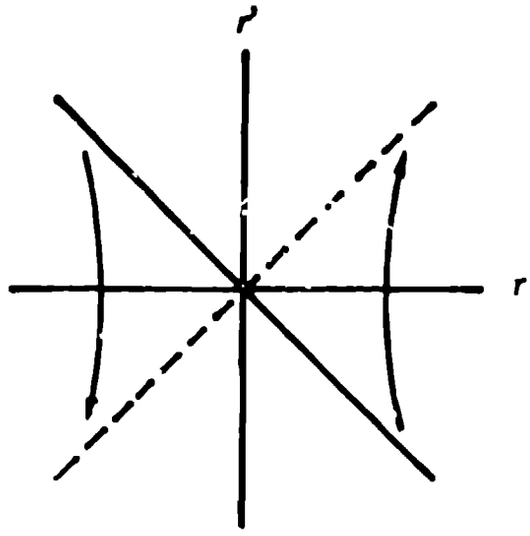

(b)

RF INJECTOR AND 500-MeV LINAC CONFIGURATION

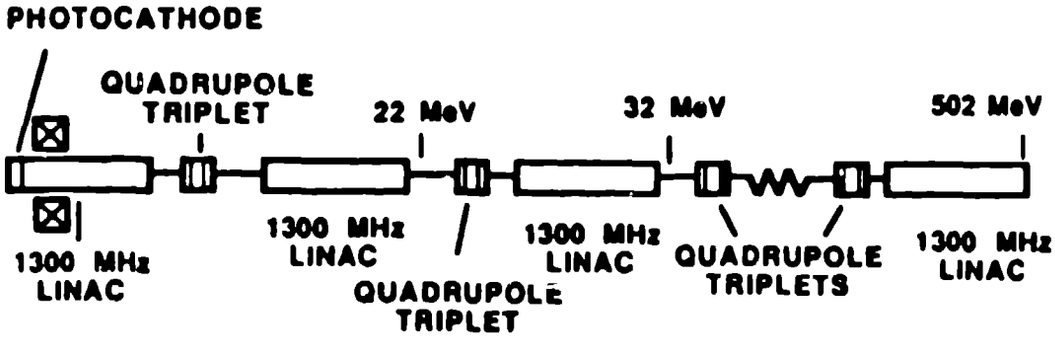

ENERGY SPREAD AND EMITTANCE